

Thermodynamics of a mixed quantum-classical Heisenberg model in two dimensions

J. Leandri, Y. Leroyer, S.V. Meshkov and Y. Meurdesoif
Centre de Physique Théorique et de Modélisation de Bordeaux
Université Bordeaux I, CNRS, Unité Associée 1537
19 rue du Solarium, 33174 Gradignan Cedex, France
 and

O. Kahn, B. Mombelli and D. Price
Laboratoire des Sciences Moléculaires
Institut de Chimie de la Matière Condensée de Bordeaux
CNRS, UPR 9048
Avenue Albert Schweitzer, 33608 Pessac Cedex, France

We study the planar antiferromagnetic Heisenberg model on a decorated hexagonal lattice, involving both classical spins (occupying the vertices) and quantum spins (occupying the middle of the links). This study is motivated by the description of a recently synthesized molecular magnetic compound. First, we trace out the spin $\frac{1}{2}$ degrees of freedom to obtain a fully classical model with an effective ferromagnetic interaction. Then, using high temperature expansions and Monte Carlo simulations, we analyse its thermal and magnetic properties. We show that it provides a good quantitative description of the magnetic susceptibility of the molecular magnet in its paramagnetic phase.

The Heisenberg model [1] has a long history and has been extensively studied throughout these last thirty years. While it is exactly solvable in one dimension [2] in some of its versions, it is only through approximate methods that quantitative information can be obtained in higher dimensions. High and low temperature expansions [3,4], Monte Carlo simulations [5,6] and renormalisation group calculations [7,8] have been widely developed and give now a precise account of the critical regime of the model. However, little has been done in the various specific contexts which are now realized in the magnetic molecular materials.

For instance, the compound $(\text{NBu}_4)_2\text{Mn}_2[\text{Cu}(\text{opba})]_3 \cdot 6\text{DMSO} \cdot \text{H}_2\text{O}$, recently synthesized by H.O. Stumpf *et al* [9], exhibits a transition at $T_c = 15\text{K}$ towards an ordered state. The structure of this material can be schematically described by a superposition of layers of hexagonal lattices with the Mn^{II} ions occupying the vertices and the Cu^{II} ions occupying the middle of the links, as shown in Fig. 1. The interplane-coupling is small, so that the spin system can be considered two-dimensional. In the plane, the nearest neighbour Mn-Cu ions interact through an antiferromagnetic coupling. It is interesting to determine the extent to which such a simple microscopic model with no other interaction included, can *quantitatively* describe the magnetic and thermal properties of such a complex molecular architecture. Of course, the isotropic $O(3)$ model is critical only at zero temperature [10] and the symmetry breaking at $T_c = 15\text{K}$ has presumably its origin in a slight spin anisotropy and/or a small interplane coupling. However, one expects for $T \gg T_c$ that the properties of the material are well described by the two-dimensional isotropic antiferromagnetic spin $\frac{1}{2}$ - spin $\frac{5}{2}$ interaction. This is the problem we investigate in this paper.

We denote by $\mathbf{S}_j^{(\text{Mn})}$ the spin $\frac{5}{2}$ operator associated with the Mn ion at site j , and by $\mathbf{S}_i^{(\text{Cu})}$ the spin $\frac{1}{2}$ operator corresponding to the Cu ion at site i in the middle of a link of the honeycomb lattice. The antiferromagnetic interaction is represented by the Heisenberg hamiltonian

$$\mathcal{H} = J \sum_{\langle i,j \rangle} \mathbf{S}_i^{(\text{Cu})} \cdot \mathbf{S}_j^{(\text{Mn})} - g_1 \mu_B H \sum_{j=1}^{N_S} S_j^{z(\text{Mn})} - g_2 \mu_B H \sum_{i=1}^{N_L} S_i^{z(\text{Cu})} \quad (1)$$

where J is positive, H is the external magnetic field, $\langle i,j \rangle$ stands for a pair of nearest neighbour spins, N_S is the number of sites and N_L is the number of links on the honeycomb lattice ($N_L = 3/2 N_S$). The spin $\frac{5}{2}$ operator can be approximated by a *classical* spin \mathbf{S} where \mathbf{s} is a unit classical vector and $S = \sqrt{\frac{5}{2}(\frac{5}{2} + 1)}$, whereas the spin $\frac{1}{2}$ operators are expressed in terms of the Pauli matrices, $\mathbf{S}^{(\text{Cu})} = \frac{1}{2} \boldsymbol{\sigma}$. Since the quantum spin sites are not directly coupled to each other, one can trace out the quantum spin dependence to get a completely classical partition function

$$Z(T, H) = \int \mathcal{D}\mathbf{s} \left\{ \prod_{\langle ij \rangle} 2 \cosh \left(\left\| -\frac{1}{2} \beta J S (\mathbf{s}_i + \mathbf{s}_j) + \alpha_2 H \hat{\mathbf{e}}_z \right\| \right) \right\} \exp \left(\alpha_1 H \sum_{i=1}^{N_S} s_i^z \right) \quad (2)$$

where we have defined $\alpha_1 = S \beta g_1 \mu_B$, $\alpha_2 = \frac{1}{2} \beta g_2 \mu_B$, $\mathcal{D}\mathbf{s} = \prod_{j=1}^{N_S} \sin \theta_j d\theta_j d\varphi_j$ and $\|\mathbf{X}\|$ stands for the length of vector \mathbf{X} . The indices i and j now label the *classical* spins located at the vertices of the honeycomb lattice.

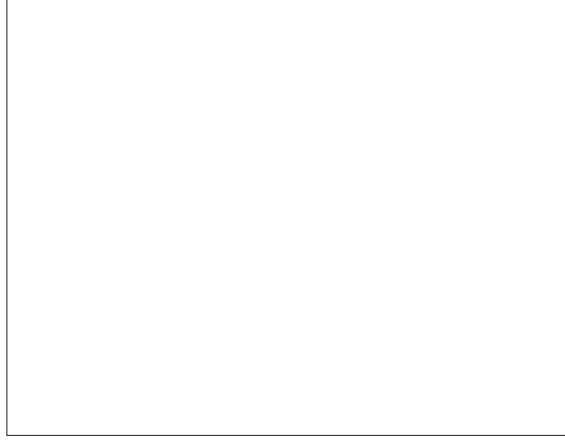


FIG. 1. Structure of a layer in $(\text{NBu}_4)_2\text{Mn}_2[\text{Cu}(\text{opba})]_3 \cdot 6\text{DMSO} \cdot \text{H}_2\text{O}$

The partition function of Eq.(2) will now be treated by the standard techniques of high temperature expansion and Monte Carlo simulation to extract quantitative information on the system.

In zero magnetic field, the partition function becomes

$$Z(T, 0) = \int \mathcal{D}\mathbf{s} \left\{ \prod_{\langle ij \rangle} 2 \cosh\left(\frac{1}{2}\beta JS \|\mathbf{s}_i + \mathbf{s}_j\|\right) \right\} \quad (3)$$

We get an effective *ferromagnetic* interaction between the classical spins :

$$-\beta \mathcal{H}_{\text{eff}} = \sum_{\langle i,j \rangle} \ln [2 \cosh(\frac{1}{2}\beta JS \|\mathbf{s}_i + \mathbf{s}_j\|)] \quad (4)$$

We can perform a high temperature expansion of the partition function of Eq.(3). By using the star graph technique [4], we have derived the expansion of $\ln Z(T, 0)$ up to the 30th order in the variable $K = \frac{1}{2}\beta JS$. For the specific heat we obtain the following result :

$$\begin{aligned} C_V = N_L k_B \left[2K^2 - \frac{10}{3} K^4 + 4K^6 - \frac{8326}{2025} K^8 + \frac{3676}{945} K^{10} - \frac{2963432}{893025} K^{12} + \frac{43060432}{21049875} K^{14} \right. \\ + \frac{1084428794}{1915538625} K^{16} - \frac{50703530596}{9577693125} K^{18} + \frac{174515087256364}{13540176324675} K^{20} - \frac{10010372498598008}{417635308715625} K^{22} \\ + \frac{1712584839620191683704}{43895559122555765625} K^{24} - \frac{1634086374908287292656}{27958094579597056875} K^{26} \\ \left. + \frac{218588272951603892608}{2641543327626328125} K^{28} - \frac{9205154548418515452736832}{81777426645321391359375} K^{30} \right] \quad (5) \end{aligned}$$

According to Eq.(2), the zero-field susceptibility, defined by $\chi = \frac{k_B T}{V} \left. \frac{\partial^2 \ln Z}{\partial H^2} \right|_{H=0}$, can be expressed as :

$$\chi = \frac{k_B T}{V} \frac{1}{Z(T, 0)} \int \mathcal{D}\mathbf{s} \left\{ \prod_{\langle ij \rangle} 2 \cosh W_{ij} \right\} \left[\left(\alpha_1 \sum_i s_i^z + \alpha_2 \sum_{\langle ij \rangle} \bar{s}_{ij}^z \right)^2 + \alpha_2^2 \sum_{\langle ij \rangle} Q_{ij} \right] \quad (6)$$

where $W_{ij} = \frac{1}{2}\beta JS \|\mathbf{s}_i + \mathbf{s}_j\|$, $W_{ij}^z = -\frac{1}{2}\beta JS(s_i^z + s_j^z)$, $\bar{s}_{ij}^z = \tanh(W_{ij}) W_{ij}^z / W_{ij}$ and

$$Q_{ij} = \frac{\tanh(W_{ij})}{W_{ij}} \left[1 - \left(\frac{W_{ij}^z}{W_{ij}} \right)^2 \right] + \left(\frac{W_{ij}^z}{W_{ij}} \right)^2 - (\bar{s}_{ij}^z)^2$$

The high temperature expansion of χ can be obtained in two independent ways : first by expanding the partition function of Eq.(2) both in powers of K and H and retaining the coefficient of H^2 ; second, through an expansion of

the correlation functions which occur in Eq.(6). Up to the 7th order, we apply both methods in order to validate our results. By using the second approach, more tractable at higher orders, we have obtained the following series, up to the order 11 :

$$\begin{aligned}
T\chi = \frac{N_L \mu_B^2}{V k_B} & \left[\frac{2}{9} g_1^2 S^2 + \frac{1}{4} g_2^2 - \frac{2}{3} g_1 g_2 S K + \frac{2}{9} (g_1^2 S^2 + g_2^2) K^2 \right. \\
& - \frac{2}{27} g_1 g_2 S K^3 - \frac{1}{15} g_2^2 K^4 - \frac{8}{405} g_1 g_2 S K^5 + \left(\frac{2}{225} g_1^2 S^2 + \frac{533}{8505} g_2^2 \right) K^6 \\
& + \frac{2}{8505} g_1 g_2 S K^7 - \left(\frac{4}{2835} g_1^2 S^2 + \frac{5683}{127575} g_2^2 \right) K^8 - \frac{4}{4725} g_1 g_2 S K^9 \\
& \left. + \left(\frac{524}{893025} g_1^2 S^2 + \frac{19912}{601425} g_2^2 \right) K^{10} + \frac{7108}{49116375} g_1 g_2 S K^{11} \right]
\end{aligned} \tag{7}$$

In order to improve the range of validity of the expansions (Eqs.(5,7)) we performed a Padé approximant extrapolation toward low temperatures (large K values). For both series we get good stability of the Padé table. The results will be presented below.

We performed a self-consistent check of our results by means of a Monte Carlo simulation of the effective classical model (Eq.(4)). The various observables can be expressed as ensemble averages with respect to the Boltzmann weight $1/Z(T,0)e^{-\beta \mathcal{H}_{\text{eff}}}$. For instance, if we define $E = -k_B T \sum_{\langle i,j \rangle} W_{ij} \tanh(W_{ij})$ which is the energy of the quantum spins for a fixed configuration of the classical ones, we find that the internal energy is simply given by $\langle E \rangle_{\mathcal{H}_{\text{eff}}}$ and the specific heat by

$$C_V = k_B \beta^2 \left[\langle E^2 \rangle_{\mathcal{H}_{\text{eff}}} - \langle E \rangle_{\mathcal{H}_{\text{eff}}}^2 \right] + k_B \langle \Phi \rangle_{\mathcal{H}_{\text{eff}}} \quad \text{with} \quad \Phi = \sum_{\langle i,j \rangle} \left[\frac{W_{ij}}{\cosh(W_{ij})} \right]^2 \tag{8}$$

Similarly, from Eq.(6) the susceptibility can be expressed as a sample average. We have used the Wolf algorithm [6] adapted to our effective Boltzmann weight, on lattices of size increasing with K , up to 2^{16} hexagons for $K = 5$.

In Fig. 2 we have plotted the specific heat as a function of K . The data points correspond to the Monte Carlo simulation and the continuous line to the highest order diagonal Padé approximant of the high temperature expansion. The first remarkable feature is the well marked knee-hump variation of C_V as the temperature decreases. One can understand this effect in the following way. At very low temperature, the system is dominated by the effective ferromagnetic interaction between the classical spins. For the purely classical Heisenberg model, one expects a peak at low temperature in the specific heat [11], corresponding to the crossover between the low temperature critical regime and the high temperature uncorrelated one.

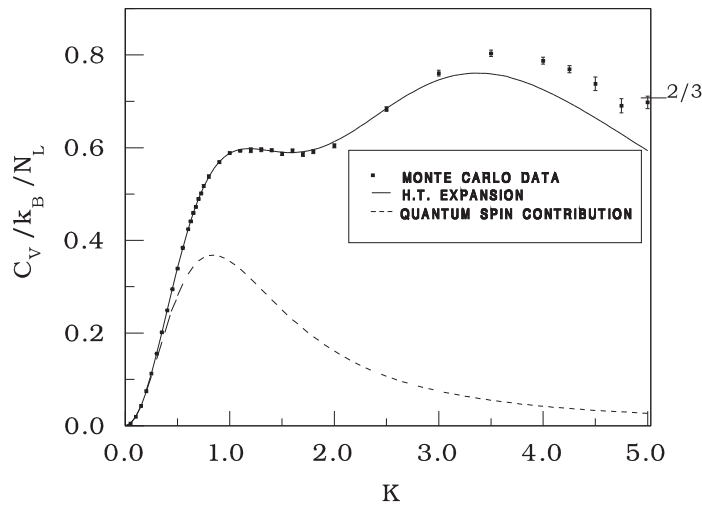


FIG. 2. Specific heat $C_V/N_L k_B$ versus $K = 1/2\beta JS$: The Monte Carlo results are represented by squares, the solid line shows the Diagonal (7,7) Padé approximant corresponding to the high temperature series of Eq.(5) and the contribution of the quantum spins obtained from Eq.(9) is shown as a dashed line. The zero-temperature ($K \rightarrow \infty$) limit, $C_V/N_L k_B = 2/3$, is indicated.

The hump observed in Fig. 2 near $K = 4$ corresponds to this effect. As T increases, the classical spin system goes rapidly to a disordered state, whereas the quantum spins remain locally coupled to their classical neighbours. The knee at $K = 1$ corresponds to this local antiferromagnetic order. This effect can be quantitatively confirmed by the following calculation. Assuming that the classical spins are completely random leads to $\langle E^2 \rangle = \langle E \rangle^2$ in Eq.(8) and

$$C_v = k_B \langle \Phi \rangle_{\text{disordered}} = 8N_L k_B K^2 \int_0^1 \frac{y^3}{\cosh^2(2Ky)} dy \quad (9)$$

This function, displayed in Fig. 2 (dashed line), exhibits a peak exactly under the bump observed in the full C_v .

The other feature which emerges from Fig. 2 is the spectacular agreement of the series expansion with the Monte Carlo results up to $K \simeq 3$ and the ability of this series to reproduce the double-bump structure.

We obtain the same perfect agreement of both our methods for the magnetic susceptibility up to $K = 3$. In Fig. 3, we have plotted (solid line) the (6,6) Padé approximant of the series Eq.(7) as a function of temperature, in a range which corresponds to $0 < K < 1.2$. The data points correspond to the experimental results which will be discussed below. The shape of this curve can be explained as follows. Here again there are two physically different and competing correlation effects. The first one, due to the antiferromagnetic spin compensation, leads to a decrease of the susceptibility, more pronounced at lower temperature. The other contribution, due to the ferromagnetic correlation of the classical spins, induces a divergence at $T = 0$.

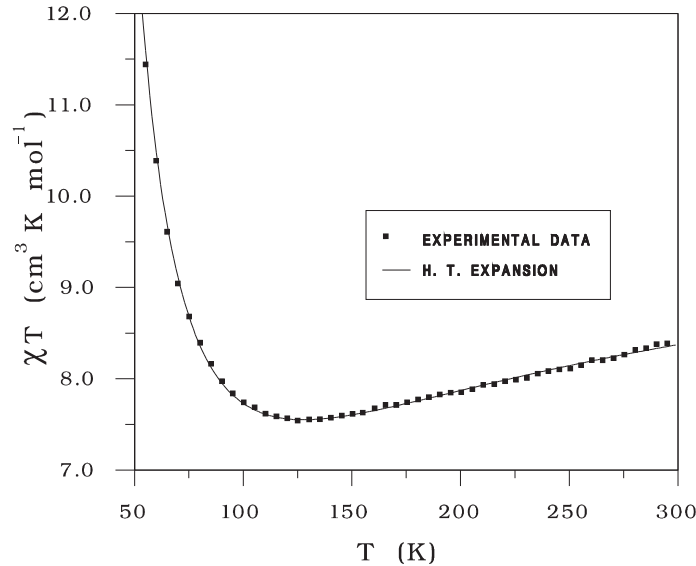


FIG. 3. Magnetic susceptibility times temperature χT in units of $\text{cm}^3 : \text{K} : \text{mol}^{-1}$ versus T in Kelvin: The experimental data (squares) are taken from [9]; the solid line corresponds to the diagonal (6,6) Padé approximant based on the high temperature series Eq.(7) with $J = 47.6$ K, $g_1 = 2.0$, $g_2 = 2.2$.

According to universality, we expect the critical behaviour at zero temperature to be described by the non-linear σ -model. At low temperature the effective interaction Eq.(4) reduces to

$$\mathcal{H}_{\text{eff}} \simeq -\frac{1}{2}JS \sum_{\langle ij \rangle} \|\mathbf{s}_i + \mathbf{s}_j\| \approx \text{const} + \frac{1}{8}JS \sum_{\langle ij \rangle} \theta_{ij}^2$$

which corresponds to the low temperature limit of the ordinary classical Heisenberg model on the honeycomb lattice with the ferromagnetic exchange constant $J^* = \frac{1}{4}JS$. The long wave-length expansion leads us further to the total effective energy in the form of the non-linear σ -model Hamiltonian

$$H_\sigma = \frac{JS}{4\sqrt{3}} \frac{1}{2} \int (\partial_\alpha \mathbf{n}) (\partial_\alpha \mathbf{n}) d^2r \quad (10)$$

where $\mathbf{n}(\mathbf{r})$ is the three dimensional unit vector field on the two dimensional plane \mathbf{r} . As an immediate consequence from the quadratic expansion we have the magnon contribution to the total energy per classical spin which is linear in T :

$$\overline{E} \approx -\frac{3}{2}JS + k_B T$$

leading to the constant specific heat at low temperature $C_V = \frac{2}{3}N_L k_B$. One can see in Fig. 2 that our Monte Carlo data are compatible with this value.

As another consequence, we can borrow the low temperature behaviour of the magnetic susceptibility from the renormalisation group results [8,12] for the non-linear σ -model of Eq.(10)

$$\chi = \text{const} \cdot T^3 \exp \left[\frac{4\pi}{k_B T} \frac{JS}{4\sqrt{3}} \right] = \text{const} \cdot T^3 \exp \left[\frac{2\pi}{\sqrt{3}} K \right] \quad (11)$$

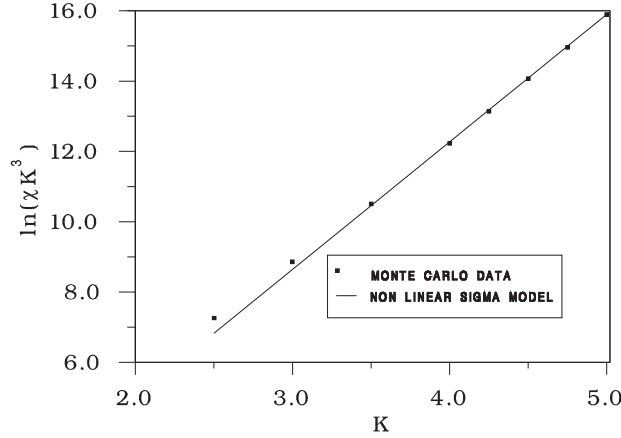


FIG. 4. $\ln(\chi K^3)$ versus K : The squares correspond to Monte Carlo results while the solid line shows the prediction of Eq.(11) of the non-linear σ -model.

In Fig. 4 we have plotted the low temperature Monte Carlo data for $\ln(K^3\chi)$ as a function of K . The straight line corresponds to the behaviour of Eq.(11). We obtain very good agreement, thereby confirming that at our lowest temperatures, we are well inside the expected universality region and the size of our simulated lattices is large enough.

These results show that our series expansions constitute a reliable parametrisation of the specific heat and the magnetic susceptibility of the model up to $K \approx 3$. We can now apply this parametrisation to the experimental data [9] We have fitted the product $T\chi$ as a function of the temperature in the range $60K \leq T \leq 300K$ with J , g_1 and g_2 as free parameters. The result is shown in Fig. 3, with the best-fit parameters given by $J = 47.6K$, $g_1 = 2.0$ and $g_2 = 2.2$. We observe excellent agreement with the experimental data, confirming that the high temperature magnetic properties of this compound are well described by our model. Furthermore, these values of the parameters are very close to those obtained for both Cu-Mn pairs [13] and chains [9,14] with the same bridging network. The weakly pronounced minimum observed in Fig. 3 for $T \approx 120K$ has its origin in the local antiferromagnetic ordering discussed above.

The material exhibits a ferromagnetic transition at $T_c = 15K$ that the isotropic model cannot describe. To give an account of this nonzero-temperature critical behaviour the Hamiltonian must be generalized to include spin anisotropy and three-dimensional effects [15], a modification which we are now investigating. However, it is amazing that the agreement between the experimental data and the model persists down to rather low temperatures ($T \approx 20K$), close to the measured T_c .

Acknowledgements

S.V. M. thanks V.A. Fateev and A.I.B. Zamolodchikov for helpful discussions.

-
- [1] W. Heisenberg, *Z.Physik* **49**, (1928) 619
 - [2] M.E. Fisher, *Am. J. Phys.* **32**, (1964) 343
 - [3] G.S. Rushbrooke, G.A.Baker and P.J. Wood in "Phase transitions and critical phenomena", vol. 3, p. 246, C. Domb and M.S. Green editors, (Academic Press, 1974).

- [4] S. McKenzie, *NATO advanced Study Series : Phase Transitions* **B72**, (1980) 271
- [5] for a review, see K. Binder, Monte Carlo simulations and statistical mechanics, Springer Verlag, 1992.
- [6] U. Wolf, *Phys. Rev. Lett.* **62**, (1989) 361
- [7] A.M. Polyakov, *Phys. Lett.* **59B**, (1975) 79
A.A.Migdal, *Ah. Eksp. Teor. Fiz.* **69**, (1975) 810
- [8] E. Brézin and J. Zinn-Justin, *Phys. Rev. Lett.* **36**, (1976) 691
- [9] H.O. Stumpf, Yu Pei, O. Kahn, J. Sletten and J.P. Renard, *J. Am. Chem. Soc.* **115**, (1993) 6738
D. Price and O. Kahn, unpublished results.
- [10] N. D. Mermin and H. Wagner, *Phys. Rev. Lett.* **17**, (1966) 1133
- [11] This bump is visible for instance in the results of the test of our simulation method performed on the purely classical Heisenberg model on a square lattice. See also A. Cuccoli, V. Tognetti and R. Vaia *Phys. Rev.* **B52**, (1995) 10221 (in the case of 1% anisotropy) and S.H. Shenker and J. Tobochnik, *Phys. Rev.* **B22**, (1980) 4462.
- [12] M. Falcioni and A. Treves, *Nucl. Phys.* **B265**, ([FS15] 1986) 671
- [13] C. Mathomère, O. Kahn, J.C. Daran, H. Hilbig and F. H. Köble *Inorg. Chem.* **32**, (1993) 4057
- [14] R. Georges, J. Curély, J.C. Gianduzzo, Q. Xu, O. Kahn, Y. Pei, *Physica B+C* **77**, (1988) 153
- [15] R.A.Pelcovits and D.R.Nelson, *Phys. Lett.* **A57**, (1976) 23
S. Hikami and T. Tsuneto, *Prog. Theor. Phys.* **63**, (1979) 387